EPJ Web of Conferences **63**, 02019 (2013)
DOI: 10.1051/epjconf/ 20136302019

Elastic scattering and heavy residue production in the collisions ^{6,7}Li+^{64}Zn around the Coulomb barrier

P.Figuera[1,a], A.Di Pietro[1], E.Strano[1,2], M.Fisichella[1], M.Lattuada[1,2], M.Milin[3], A.Musumarra[1,2], V. Ostashko[4], M.G.Pellegriti[1], G.Randisi[1,2], V.Scuderi[1,2], D. Torresi[1,2], and M.Zadro[5]

[1]INFN Laboratori Nazionali del Sud, Catania, Italy
[2]Dipartimento di Fisica ed Astronomia Universita' di Catania, Catania, Italy
[3]Department of Physics University of Zagreb, Zagreb, Croatia
[4]KINR, Kiev, Ukraine
[5]Ruder Boskovic Institute, Zagreb, Croatia

Abstract. Elastic scattering angular distributions and heavy residue production cross sections have been measured at different energies around the Coulomb barrier for the systems ^{6,7}Li+^{64}Zn. Optical model fits of the elastic angular distributions were performed using a renormalized double folding potential and absence of usual threshold anomaly in the optical potential was found. Excitation functions for heavy residue production have been measured using an activation technique. Comparison of the data with the results of different calculations show that complete fusion is the dominant reaction mechanism above the barrier, whereas the heavy residue yield below the barrier is mainly due to incomplete fusion and transfer.

1 Introduction

The study of nuclear collisions involving weakly bound or halo nuclei, at energies around the Coulomb barrier, had a considerable interest in the last decade, since the peculiar structure of such nuclei can deeply affect the reaction mechanisms (see e.g. [1]). One expects that direct processes like breakup and transfer are important due to the halo or cluster structure of the weakly bound projectiles. Coupling to continuum effects are expected to have an important role on elastic scattering (see e.g. [2-9]) and fusion (see e.g. [10-11] and references therein) around the barrier. Due to the presence of a repulsive polarization potential, associated to coupling to continuum, the usual threshold anomaly in the optical potential may disappear in such collisions. The study of fusion reactions is complicated by the fact that, in addition to complete fusion (CF), one may have incomplete fusion (ICF) processes following breakup of the weakly bound projectile. In order to further investigate on these topics, we measured elastic scattering angular distributions and heavy residue (HR) production cross sections at several energies around the Coulomb barrier for the systems ^{6,7}Li+^{64}Zn. The experiments were performed at the Tandem of the Laboratori Nazionali del Sud in Catania.

2 Elastic scattering angular distributions

Elastic scattering angular distributions in a wide angular range ($20^o<\theta_{c.m.}<170^o$) were measured at several energies around the barrier, using 5 ΔE(10 μm)-E(200 μm) silicon telescopes mounted on a rotating arm. The angular distributions were reproduced within the optical model

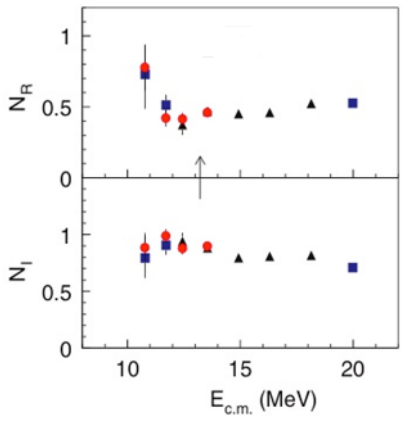

Figure 1. Renormalization coefficients for the real and imaginary part of the potential in the collision ^{6}Li+^{64}Zn. The arrow indicates the position of the Coulomb barrier. Different symbols refer to independent experiments. See text for details.

[a] Corresponding author: figuera@lns.infn.it

(OM) using a renormalized double folding potential for the real and imaginary part and leaving the renormalization coefficients as free parameters in the fits. The energy dependence of the real and imaginary renormalization coefficients shows absence of the usual threshold anomaly for both systems, as already observed in other collisions involving ^{6,7}Li (see e.g. [5-8]). As an example, we show in figure 1 the result for the ^{6}Li+^{64}Zn case [8]. Similar conclusions were obtained using a Woods-Saxon imaginary potential.

3 Heavy residue production

The heavy residue production cross sections have been measured by using an activation technique, detecting off-line the atomic X-rays emitted after the electron capture decay of the residues (see e.g. [12,13]). For each bombarding energy, the beam was first crossing a thin Au foil and was then impinging on a ^{64}Zn target evaporated on a catcher, which stopped all produced HR. Rutherford scattering by the thin Au foil was monitored by two Si detectors, in order to get information on the beam current as function of time during the activation. For each bombarding energy, the decay of the implanted HR was monitored off-line using two identical lead shielded Si(Li) detectors. An X-ray detection efficiency of (7.3±0.7)% was obtained with Monte Carlo simulations and confirmed using a calibrated ^{55}Fe source. A typical X-ray spectrum, measured for the collision ^{6}Li+^{64}Zn about 3 months after the end of the activation, is shown in figure 2. The X-ray spectra do not allow isotopic

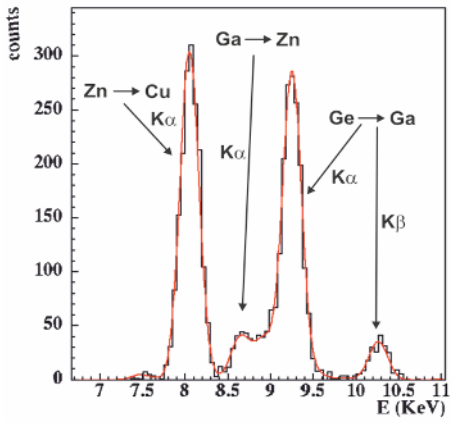

Figure 2. Typical off-line X-ray spectrum, for the collision ^{6}Li+^{64}Zn at 20 MeV, detected about 3 months after the end of the activation.

identification of the emitted HR. However, this was obtained following the activity of each peak as function of time, since different isotopes have different half lives. As an example, in figure 3 we show the activity of the Ga peak for the reaction ^{6}Li+^{64}Zn a $E_{c.m.}$= 28.3 MeV. The production cross sections of the different isotopes have been obtained, as in [12,13], analysing these activity curves and taking into account different factors such as: detection efficiency, fluorescence probability, X-ray absorption in the catcher and target foils, beam current as function of time during activation.

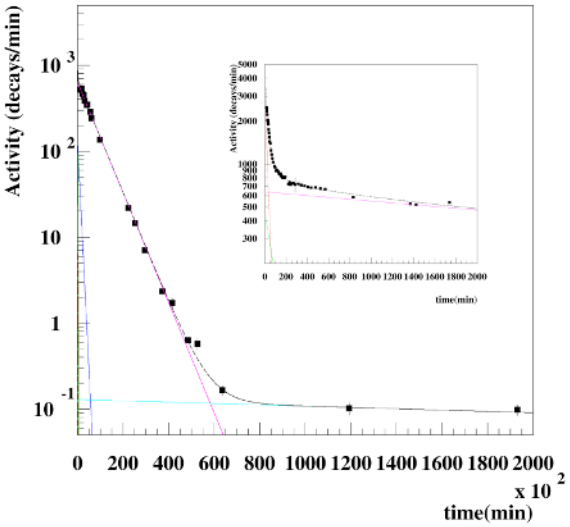

Figure 3. Activity of the Ga peak as function of time for the collision ^{6}Li+^{64}Zn at $E_{c.m.}$= 28.3 MeV. The contribution of Ga isotopes having different half lives is shown by the different straight lines.

Excitation functions for HR production are shown in figures 4 and 5, together with the results of single barrier penetration (SBP) and coupled channels (CC) calculations including the excitation of different states of projectile and target. As one can see, both calculations reproduce the data above barrier but fail below it. A possible reason for that would be the presence of reaction mechanisms different than complete fusion in

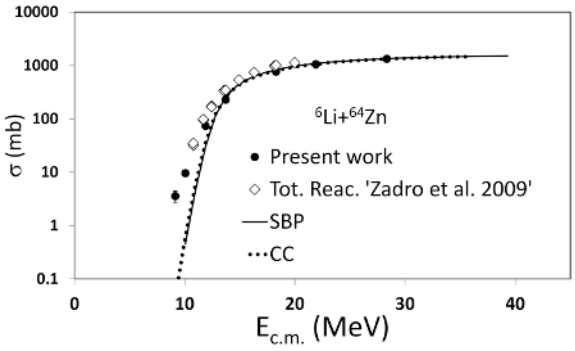

Figure 4. Cross sections for heavy residue production (closed circles) and total reaction (open diamonds) for ^{6}Li+^{64}Zn. The total reaction data are from ref. [8]. The continuous and dotted lines represent single barrier penetration and CC calculations for complete fusion. See text for details.

the low energy region. Indeed ^{6}Li and ^{7}Li have pronounced α-d and α-t cluster structures in the ground state with corresponding separation energies S_{α}=1.47 and S_{α}=2.47 MeV respectively. Therefore, one can expect reactions were only an alpha particle, a deuteron or a tritium are captured by the target. This may happen in two different ways (see e.g. [15-17]): breakup followed by incomplete fusion (ICF) or a direct cluster transfer (DCT). The use of an activation technique, such as the one of the present study, avoids the energy threshold problems linked with the direct detection of the HR.

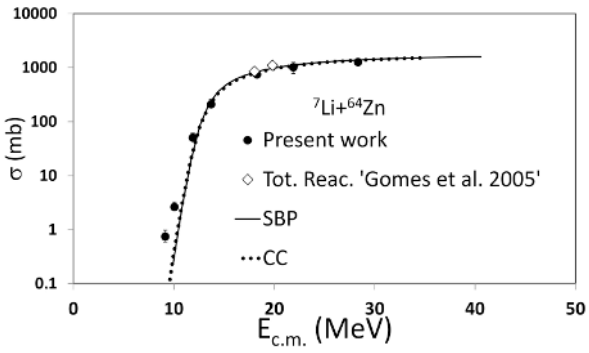

Figure 5. Cross sections for heavy residue production (closed circles) and total reaction (open diamonds) for ^{7}Li+^{64}Zn. The total reaction data are from ref. [14]. The continuous and dotted lines represent single barrier penetration and CC calculations for complete fusion. See text for details.

At the same time, however, it does not give access to any kind of kinematical information, therefore the involved reaction mechanisms can be inferred only from the experimental relative yield of the different heavy residues. For this reason, the ICF and DCT processes cannot be distinguished in the present study since the excitation energies reached in the two mechanisms (and in turn the associated relative yield of the residues) are expected to be very similar. In figure 6 the experimental relative yield of heavy residues for ^{6}Li+^{64}Zn is compared with the predictions of the statistical model code Cascade [18] for complete fusion and for the capture of a deuteron or an α particle. Used excitation energies following the d or α capture were estimated assuming an ICF mechanisms where the available fragment-target centre of mass energy before ICF occurs is: $(E_{c.m.}-S_{\alpha})\times(m_{clu}/m_{proj})$. Here $E_{c.m.}$ is the initial centre of mass energy of the ^{6}Li+^{64}Zn system, S_{α} is the α separation energy of the projectile and m_{clu} and m_{proj} are the masses of the captured cluster and of the projectile respectively. Excitation energies estimated for a cluster transfer process were only slightly smaller than the ones for ICF giving basically the same relative yield as for ICF. At energies well above the Coulomb barrier (V_C~13 MeV [8]) the HR relative yield is similar to the CF predictions. Therefore, in this energy range complete fusion appears to be the dominating mechanisms, although the extra yield for ^{65}Zn and ^{65}Ga could indicate the presence of different mechanisms such as deuteron capture. At energies below the Coulomb barrier, contrary to the Cascade predictions for CF, most of the HR yield is due to ^{65}Zn and ^{65}Ga. This indicates that mechanisms different than CF are dominating. Apart from deuteron capture, ^{65}Zn and ^{65}Ga can also be populated in 1n and 1p transfer reactions respectively. Indeed, in [20,21] it is suggested that in ^{6,7}Li induced collisions breakup following single nucleon transfer is an important channel. Finite range DWBA calculations for these single nucleon transfer reactions, performed with the code Fresco [19], predict cross sections of the same order as the measured ones below the barrier whereas, above the barrier, the ^{65}Zn and ^{65}Ga yields are larger than the Fresco

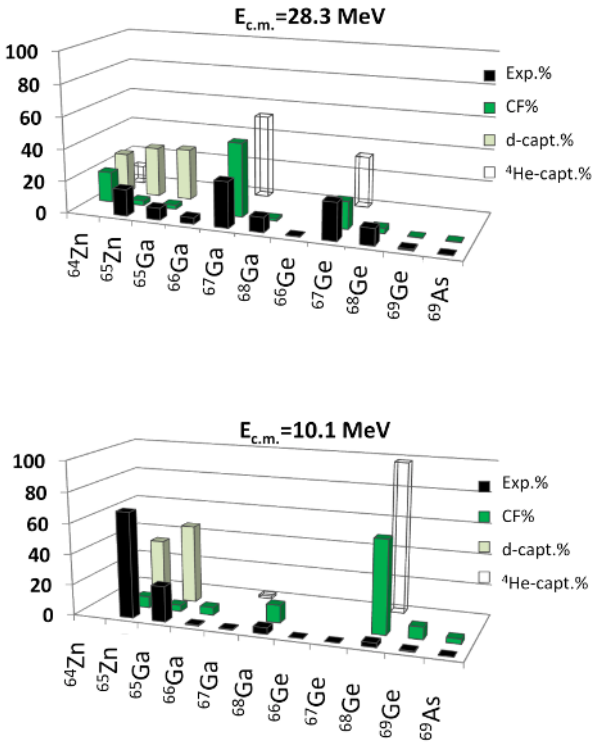

Figure 6. Experimental heavy residue relative yield for ^{6}Li+^{64}Zn compared with the prediction of statistical model calculations for complete fusion and deuteron or α capture. See text for details.

predictions. Similar results were also reached for the^{7}Li+^{64}Zn system, were the experimental HR relative yield is similar to the one predicted for CF above the barrier, but not below the barrier. As an example, in figure 7 the experimental HR relative yield for ^{7}Li+^{64}Zn is compared with the Cascade predictions for complete fusion and triton or α capture at low energy. As one can see in figure 7, at low energy, the HR production is once more dominated by those residues (^{66}Ga an^{65}Zn) which are expected in tritium capture and 1n transfer reactions. Indeed, the presence of 1n transfer reactions for the present colliding system is clearly seen in [9].

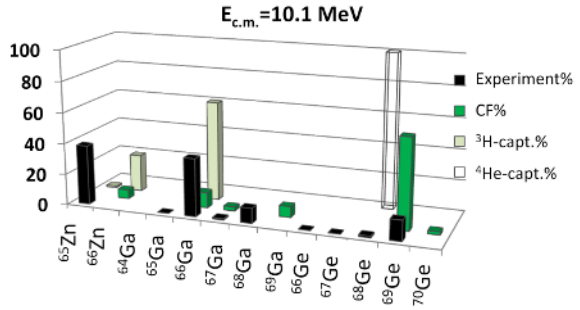

Figure 7. Experimental heavy residue relative yield for ^{7}Li+^{64}Zn compared with the prediction of statistical model calculations for complete fusion and tritium or α capture. See text for details.

As expected and confirmed by DWBA calculations, 1p transfer producing ^{65}Ga is not observed for ^{7}Li+^{64}Zn, due to its highly negative Q_{gg}. In summary, CF appears to dominate HR production above barrier whereas, different mechanisms such as deuteron or tritium capture via ICF or DCT and single nucleon transfer dominate the HR production below the barrier. In order to understand whether our conclusion olds true also for different colliding systems involving ^{6,7}Li, we performed a similar comparison with statistical model calculations for the HR data of ^{6}Li+^{59}Co [22]. In [22] the HR excitation functions

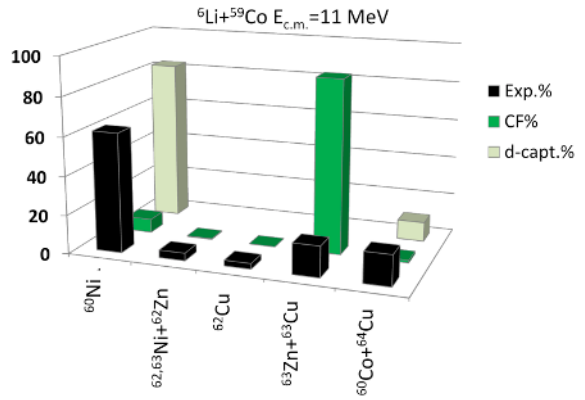

Figure 8. Experimental heavy residue relative yield for ^{6}Li+^{59}Co at $E_{c.m.}$ = 10.7 MeV from [22], compared with the prediction of statistical model calculations for complete fusion and deuteron capture. See text for details.

for the collision ^{6}Li+^{59}Co have been measured around the Coulomb barrier detecting on-line the γ rays emitted in the reactions. In figure 8 the experimental HR relative yield for ^{6}Li+^{59}Co [22] at the lowest measured energy ($E_{c.m.} \approx 11$ MeV) is compared with Cascade calculations for CF and deuteron capture. As one can see, in some cases, the summed cross sections for different HR are reported due to the fact that they were not separated in the original paper [22]. The cascade calculations have been performed as explained above for the ^{6}Li+^{64}Zn system. As already observed for ^{6}Li+^{64}Zn at low energies, although calculations for complete fusion predict a larger population for the heavier masses, most of the experimental yield is observed for the lighter ^{60}Ni and ^{60}Co (although not experimentally separated from ^{64}Cu). As shown in figure 7, these two nuclei are expected to be populated in d capture reactions and, in addition, they can also be populated by 1p and 1n transfer reactions. Therefore, also in this case, the HR yield below the barrier appears to be dominated by ICF or DCT of the deuteron and by single nucleon transfer.

4 Summary and conclusions

Elastic scattering angular distributions and heavy residue production excitation functions have been measured for the systems ^{6,7}Li+^{64}Zn. The elastic scattering angular distributions have been reproduced within the optical model using a renormalized double folding potential for the real in imaginary part. Absence of the usual threshold anomaly in the optical potential was found for both colliding systems. The heavy residue production cross sections have been measured by using an activation technique. The experimental relative yield of heavy residues was compared with the predictions of statistical model calculations. This comparison suggests that above the barrier heavy residue production is dominated by complete fusion whereas, below the barrier, other mechanisms such as ICF, DCT, and single nucleon transfer are dominating. Therefore, new experiments able to distinguish the contribution of different reaction mechanisms are necessary for a deeper understanding of fusion in collisions induced by weakly bound projectiles.

References

1. L.F. Canto at al., Phys. Rep. **424**, 1 (2006)
2. M. Cubero et al., Phys. Rev. Lett. **109,** 262701 (2012)
3. A. Di Pietro et al., Phys. Rev. Lett. **105**, 022701 (2010)
4. A. Di Pietro et al., Phys. Rev. C **85**, 054607 (2012)
5. H.Kumawat et al., Phys. Rev. C **78**, 044617 (2008)
6. J.M. Figueira et al., Phys. Rev. C **81**, 024613 (2010)
7. A.M.M. Maciel et al., Phys. Rev. C **59**, 2103 (1999)
8. M. Zadro at al., Phys. Rev. C **80**, 064610 (2009)
9. M. Zadro et al., Phys. Rev. C **87**, 054606 (2013)
10. L. F. Canto et al., Nucl. Phys., A **821**, 51 (2009)
11. P.R.S. Gomes et al., Phys. Rev. C **79**, 027606 (2009)
12. A. Di Pietro et al, Phys. Rev. C **69**, 044613 (2004)
13. V.Scuderi et al., Phys. Rev. C **84**, 064604 (2011)
14. P.R.S. Gomes et. al., Phys. Rev. C **71**, 034608 (2005)
15. A. Shrivastava et al., Phys. Lett. B **718**, 931 (2013)
16. V. Tripathi et al., Phys. Rev. C **72**, 017601 (2005)
17. F. A. Souza et al., Nucl. Phys. A **821**, 36 (2009)
18. F.Puhlhofer, Nucl. Phys. A **280**, 267 (1977)
19. I. J. Thompson, Comput. Phys. Rep. **7**, 167 (1988)
20. D. Luong et al., Phys. Lett. B **695**, 105 (2011)
21. A.Shrivastava et al., Phys. Lett. B **633**, 463, (2006)
22. C. Beck et al., Phys. Rev. C **67**, 054602 (2003)